Synthesis, surface functionalization, and properties of freestanding silicon nanocrystals

Jonathan G. C. Veinot*

Freestanding silicon nanoparticles (FS-*nc*-Si) have intriguing chemical and optical properties. The present contribution outlines known synthetic methodologies and protocols for surface functionalization. Recent advancements in tailoring the photoluminescence properties of FS-*nc*-Si and future research directions will be briefly discussed.

1. Introduction

Semiconductor nanoparticles, or quantum dots, possess size-dependent optical absorption and photoluminescent (PL) response.[1] These properties arise from confining charge carriers (quantum confinement) to nanoparticle physical dimensions that approach the Bohr radius of an electrostatically bound electron–hole pair, or exciton in the bulk material.[2] Reports outlining synthetic and property-based investigations of compound semiconductor quantum dots such as CdSe, CdS, InP, and GaAs are extensive.[3] These materials have long been prepared with well-defined size, shape, and surface chemistry.[4] For example, elaborate nanostructures such as CdSe tetrapods[4a] and highly emissive CdSe/ZnS core–shell particles[4b] have been synthesized. Partly because these well-defined materials can be prepared, quantum confinement in *direct bandgap* semiconductors is widely studied, and well understood. Furthermore, some

Department of Chemistry, University of Alberta, Edmonton, AB, Canada. E-mail: jveinot@ualberta.ca; Fax: +1-780-492-8231; Tel: +1-780-492-7206

Jonathan Veinot is an Assistant Professor at the University of Alberta (Edmonton, Canada). He received his Bachelor's Degree in Chemistry at the University of Western Ontario (London, Canada) in 1994. He subsequently carried out doctoral studies at York University (Toronto, Canada) while studying the chemical and electronic properties of cadmium sulfide nanoparticles obtaining his PhD in 1999. In 2000, Dr Veinot was awarded an NSERC Post-Doctoral Fellowship, which was applied to his investigations of organic light-emitting diodes in the Marks group at Northwestern University (Evanston, Illinois). Dr. Veinot's current research program focuses on developing new, scalable methods for preparing Group IV semiconductor and transition metal nanoparticles as well as the investigation and practical application of the size dependent properties of these materials.

Jonathan Veinot

demonstrated applications of these nanomaterials include: light-emitting diodes,[5a] single electron transistors,[5b] liquid crystals,[5c] solar cells,[5d] and fluorescent labeling.[5e] Still, compound semiconductors are not ''perfect'' because they are electrochemically active and have been found to be toxic.[6]

Unlike the II–VI and III–V materials, Si is a bioinert semiconductor that is electrochemically stable.[7] Furthermore, known methods for tailoring the surface chemistry of Si often involve the formation of robust, covalent bonds that limit surface exchange reactions.[8] For *indirect bandgap* semiconductors like Si, the lowest point of the conduction band and the highest point in the valence band occur at different wavevectors in reciprocal space hence, the *bandgap* optical transition is dipole-forbidden in the infinite crystal and photoluminescence cannot occur.[9] Consequently, in contrast to its extensive use in electronic devices bulk Si has found limited optical applications. Increased interest in shrinking electronic components has spawned an interdisciplinary field focused on size-dependent properties of nanoscale Si and tailoring the Si surface chemistry.[8,10]

Silicon nanostructures including porous silicon (*p*-Si),[8] silicon rich oxides (SROs),[11] and *freestanding* crystalline Si nanoparticles (FS-*nc*-Si) have been the focus of intense research because of their unique chemical and optical characteristics. Some of this interest arises from both scientific curiosity and the potential applications offered by the seemingly forbidden bandgap transition that leads to photoluminescence not manifested in bulk Si.

As with *direct bandgap* semiconductors, when the dimensions of an *indirect bandgap* semiconductor particle are decreased to sub-100 nm, the *bandgap* energy increases and pseudo-continuous bands become discrete energy levels. When the particle dimension nears the Bohr exciton radius (*ca.* 5 nm for silicon), quantum confinement effects emerge and PL shifts into the visible of the electromagnetic spectrum. The subject of the following review is the current status of FS-*nc*-Si research including, preparation, surface functionalization, optical properties, and future outlook.

2. Synthetic methods

It is well established from studies of compound semiconductors that many variables influence semiconductor nanoparticle

properties, and among these are size, shape, crystal structure, and surface chemistry. An *ideal* preparative method would effectively address all of these issues while also producing tangible quantities of easily purified products from readily available, non-hazardous precursors. To date, a variety of approaches have been reported for preparing FS-*nc*-Si.

Solution-based precursor reduction

Solution-based procedures involving precursor reduction are among the most attractive and widely studied of all methods for metal and semiconductor nanoparticle syntheses. They hold promise of simultaneously affording control of particle size and surface chemistry while also providing relatively large sample sizes. To date, solution syntheses of FS-*nc*-Si have been somewhat limited, doubtless a direct result of the complex solution chemistry of Si.[12] One of the earliest strategies reported in 1992 by Heath[13] used a heterogeneous reaction mixture containing sodium dispersion to simultaneously reduce $SiCl_4$ and $RSiCl_3$ (R = H and *n*-octyl) at 385 °C and >100 atm in a high-pressure bomb reactor for 3 to 7 days (Scheme 1A). The product obtained from this reaction consisted of size polydisperse particles (*d* = 2–9 nm). Selected area electron diffraction showed characteristic reflections of diamond lattice Si and infrared spectroscopy confirmed Si–O, Si–Cl and Si–H surface termination. The product was isolated by filtration and freed from the only reaction byproduct, NaCl, upon washing with water. A notable variation of this alkali metal reduction was reported by Dhas *et al.*[14] who employed sonication to simulate high pressure bomb conditions to reduce tetraethyl orthosilicate using colloidal sodium dispersion in toluene at −70 °C (Scheme 1B). This same procedure was performed with $SiCl_4$; however no details were provided. The resulting grey powder was annealed at 400 °C to afford highly agglomerated diamond lattice silicon nanoparticles with diameters of 2–5 nm in 70% yield.

Recently, heterogeneous metal reduction of $SiCl_4$ has resurfaced and was employed by Baldwin *et al.* to prepare
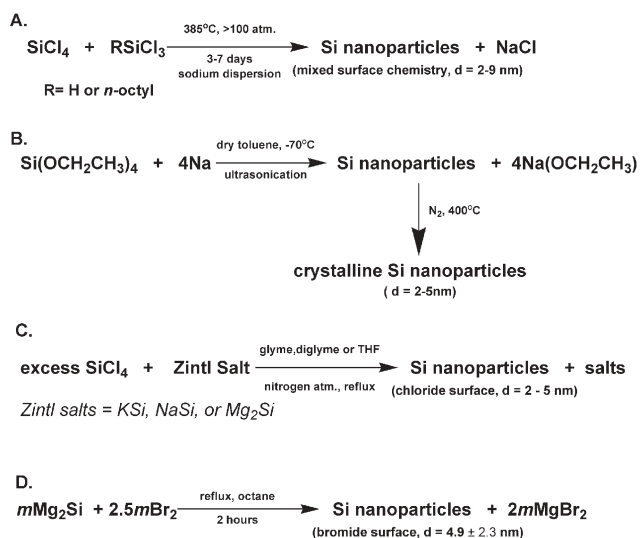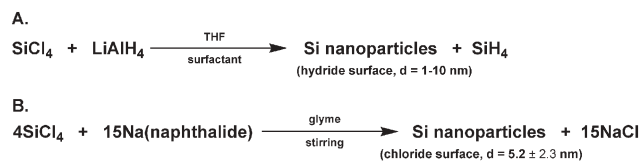
phosphorus containing, alkyl surface terminated Si nanoparticles (*d* = 2–12 nm) *via* the co-reduction of a silicon precursor in the presence of phosphorus trichloride by finely divided magnesium powder. The resulting phosphorus "doped" Si nanoparticles were melted to prepare *n*-doped Si films.[15]

Zintl salts (ASi; A = Na, K, Mg) obtained from the high temperature reaction of metals with elemental silicon have been shown to reduce $SiCl_4$ in glyme solutions to yield relatively small quantities of FS-*nc*-Si (*e.g.*, 8–85 mg). The first report in 1996 by Bley *et al.* used KSi as a reducing agent (Scheme 1C).[16] The black powder obtained from this reaction consisted primarily of an amorphous material that contained diamond lattice silicon nanoparticles and was found to be "somewhat sensitive to air and moisture". FT-IR analysis of the isolated pure nanoparticle product showed characteristic peaks for Si–O and C–H_{sat} bending and stretching frequencies. From these data and subsequent reactivity studies (*vide infra*) it was deduced that the particles produced from the redox reaction were initially chloride surface terminated and subsequent reaction with methanol during workup capped the surface with –OMe moieties. The methoxy surface termination rendered the product hydrophobic and had facilitated particle isolation from the unidentified amorphous side product *via* extraction into organic solvents. Sodium silicide (NaSi) has also found application in the solution phase synthesis of FS-*nc*-Si.[17] Replacement of alkali silicides with a more covalent, less reactive Mg_2Si yielded photoluminescent silicon nanoparticles that were readily freed from $MgCl_2$ impurities.[18] Unfortunately, because of their air sensitivity no size distribution data and only limited information regarding the chloride surface terminated nanoparticles were provided.

In a subsequent contribution, Liu *et al.* expanded the versatility of the magnesium silicide regent by showing that upon reaction with Br_2 in refluxing octane or glyme a PL material believed to be FS-*nc*-Si was produced (Scheme 1D).[19] Pettigrew *et al.*[20] later confirmed FS-*nc*-Si particles were in fact obtained from the bromine oxidation of Mg_2Si in octane. Isolation of unfunctionalized particles was not reported; however, the product was reacted with *n*-BuLi to yield an oily yellow product (0.023 g) confirmed to contain diamond lattice FS-*nc*-Si (*d* = 4.8 ± 2.0 nm) using HRTEM.

Homogeneous solution reactions have also found application in preparing FS-*nc*-Si. The reduction of $SiCl_4$ by $LiAlH_4$ has long been known to yield pyrophoric silane.[21] Wilcoxon *et al.* found that this reaction also yielded polydisperse (*d* = 2–10 nm) Si nanoparticles in "inverse micelle solutions" (Scheme 2A).[22] The product was further size selected using HPLC separation. It was assumed the resulting particle surfaces were hydride terminated, however no experimental evidence was provided. HRTEM and selected area electron diffraction of small samples were consistent with diamond lattice Si. Unfortunately, no yield data or bulk material characterization was presented.

Tilley *et al.* later used a variation of this solution reduction to prepare small quantities of small, size monodisperse FS-*nc*-Si (*d* = 1.8 ± 0.2 nm).[23] While the surface chemistry of particles obtained directly from the reaction of $SiCl_4$ with $LiAlH_4$ was not presented, particle reactivity suggests hydride surface termination (*vide infra*).

A.

$$SiCl_4 + RSiCl_3 \xrightarrow[\substack{3\text{-}7 \text{ days} \\ \text{sodium dispersion}}]{385°C, >100 \text{ atm.}} \text{Si nanoparticles} + \text{NaCl}$$

R= H or *n*-octyl   (mixed surface chemistry, d = 2-9 nm)

B.

$$Si(OCH_2CH_3)_4 + 4Na \xrightarrow[\text{ultrasonication}]{\text{dry toluene, -70°C}} \text{Si nanoparticles} + 4Na(OCH_2CH_3)$$

$$\downarrow N_2, 400°C$$

crystalline Si nanoparticles
(d = 2-5nm)

C.

$$\text{excess } SiCl_4 + \text{Zintl Salt} \xrightarrow[\text{nitrogen atm., reflux}]{\text{glyme,diglyme or THF}} \text{Si nanoparticles} + \text{salts}$$

Zintl salts = KSi, NaSi, or Mg_2Si   (chloride surface, d = 2 - 5 nm)

D.

$$mMg_2Si + 2.5mBr_2 \xrightarrow[\text{2 hours}]{\text{reflux, octane}} \text{Si nanoparticles} + 2mMgBr_2$$

(bromide surface, d = 4.9 ± 2.3 nm)

Scheme 1 Heterogeneous solution-based reduction methods for preparing freestanding silicon nanocrystals.

A.

$$SiCl_4 + LiAlH_4 \xrightarrow[\text{surfactant}]{\text{THF}} \text{Si nanoparticles } + SiH_4$$
(hydride surface, d = 1-10 nm)

B.

$$4SiCl_4 + 15Na(\text{naphthalide}) \xrightarrow[\text{stirring}]{\text{glyme}} \text{Si nanoparticles } + 15NaCl$$
(chloride surface, d = 5.2 ± 2.3 nm)

Scheme 2 Homogeneous solution-based reduction methods for preparing freestanding silicon nanocrystals.

Sodium naphthalide has also proven useful in preparing FS-*nc*-Si of varied sizes,[24,25] and surface chemistry.[24,26] This method is among the few that can claim particle shape control.[25] The general synthetic approach (Scheme 2B) reduces SiCl$_4$ with sodium naphthalide in glyme to yield a dark brown solution containing FS-*nc*-Si. The reaction is quenched upon addition of anhydrous methanol[26] or octanol[24] that was freed of the sodium chloride byproduct upon filtration. Excess naphthalene and solvent were readily removed *in vacuo*. While yields of unfunctionalized particles were not reported, isolated alkoxy surface functionalized FS-*nc*-Si with d = 4.51 nm (standard deviation, σ = 1.10 nm)[26] are obtained from this reaction as an orange solid in 30% yield. A modest variation to this procedure yielded[25] well-defined, alkyl surface terminated, tetrahedral Si particles with edge dimensions of 40–80 nm (Fig. 1B).

The versatility of Zintl salts as precursors for FS-*nc*-Si was expanded by Lee *et al.* upon demonstration that ultrasonication of glyme solutions of sodium silicide yielded polydisperse, chloride surface terminated, crystalline Si particles ($d \approx$ 1– 5 nm). This procedure afforded small quantities (*i.e.*, *ca.*
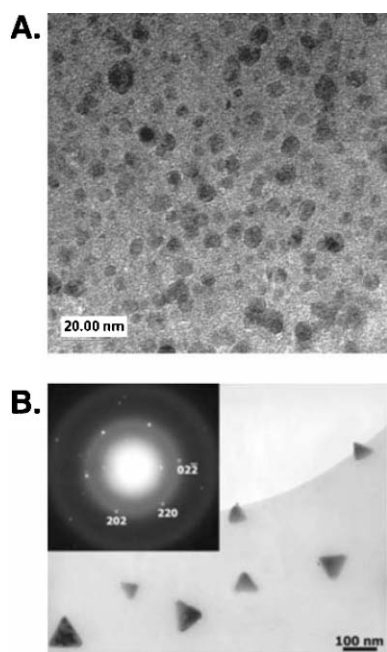

Fig. 1 A. HRTEM of *n*-octanol capped Si nanoparticles obtained from reaction of Na(naphthalide).[24] Reproduced by permission of the Royal Society of Chemistry. **B**. Bright field TEM image of Si tetrahedral obtained from reaction of SiCl$_4$ with Na(naphthalide). **Inset**: Selected area electron diffraction showing reflections characteristic of diamond lattice Si. Reprinted with permission from reference 25. Copyright 2002 American Chemical Society.

120 mg) of product in relatively high yield (*i.e.*, 60 mass%). Particles prepared from the ultrasonication of NaSi are photoluminescent emitting blue and white light depending upon sonication time.[27,28]
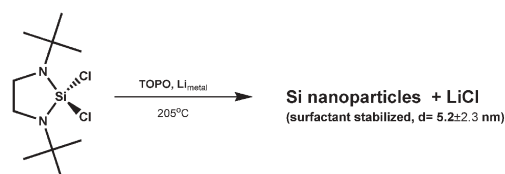
Simultaneous reduction and thermolysis of a known Metal Organic Chemical Vapour Deposition (MOCVD) precursor in trioctylphosphine oxide (TOPO) has been shown to yield FS-*nc*-Si. Scheme 3 outlines the reductive thermolysis of *N,N'*-di-*tert*-butyl-1,3-diaza-2,2-dichloro-2-silacyclopentane by lithium metal used by Rowsell and Veinot to prepare trioctylphosphine oxide (TOPO) stabilized silicon nanoparticles (d = 5.2 ± 1.2 nm).[29] FS-*nc*-Si particles were isolated as a yellow oil that exhibited broadened ^{1}H, ^{13}C, and ^{31}P NMR signals consistent with surface bonded TOPO. The product of this reaction was not readily freed from excess surfactant and surface chemistry tailoring was not straightforward.

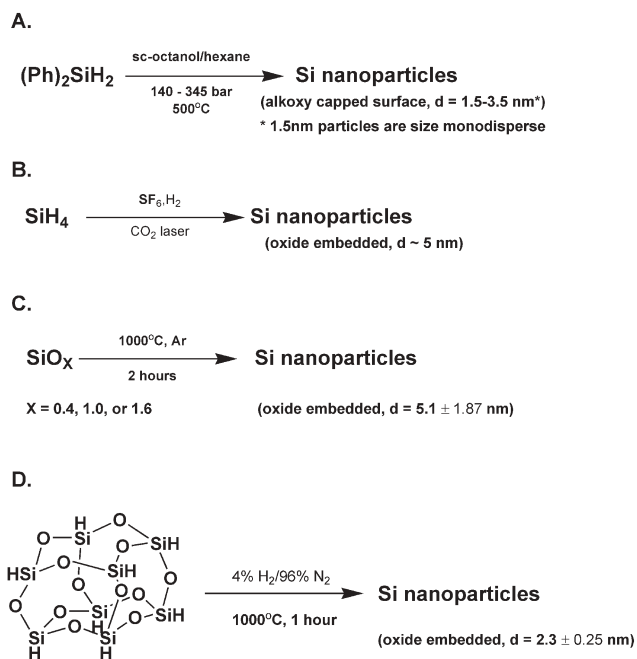**Precursor thermolysis and pyrolysis**

Solution and gas phase precursor decomposition are attractive methods for preparing semiconductor nanoparticles. The later approach has found great utility in the preparation of silicon nanomaterials. The number of reports of solution phase FS-*nc*-Si synthesis *via* precursor thermal decomposition falls far short of those of II–VI and III–V semiconductors.[29,30] Doubtless this is a result of numerous factors including the high temperatures required to "decompose" suitable precursors as well as the high reactivity of the Si surface toward solution borne reagents.

In 2001, Korgel and coworkers reported the preparation of alkoxy-functionalized FS-*nc*-Si *via* thermal degradation of diphenylsilane (Scheme 4A) in supercritical solvent mixtures of octanol and hexane with yields between 0.5% and 5% (or 0.07–1.4 mg per batch).[30] Control over the size of these crystalline particles was achieved through systematic variation of the octanol (or octanethiol) : Si ratio. In this regard, it was concluded that octanol (or octanethiol) effectively quenched the reaction and passivated the particle surface.[30,31] The smallest particles reported (*i.e.*, d = 1.5 nm) were found to be monodisperse, whereas larger particles exhibited slightly broader size distributions. Furthermore, the surfaces of FS-*nc*-Si particles prepared in this way are robustly passivated and effectively isolated resulting in the highest PL quantum yield reported to date (*vide infra*). The versatility of the super critical solution-based approach is further underscored by the reported preparation of other silicon nanomaterials including single crystalline nanowires[32] and amorphous colloids.[33]

Gas phase precursor decomposition has been used extensively in FS-*nc*-Si synthesis. The application of high temperature aerosol decomposition of SiH$_4$ to yield large

Scheme 3 Simultaneous precursor reduction–thermolysis preparation of surfactant stabilized freestanding silicon nanocrystals.

Scheme 4

A.

$(Ph)_2SiH_2$ $\xrightarrow[\substack{140 - 345 \text{ bar} \\ 500°C}]{sc\text{-octanol/hexane}}$ **Si nanoparticles**

(alkoxy capped surface, d = 1.5-3.5 nm*)

* 1.5nm particles are size monodisperse

B.

SiH_4 $\xrightarrow[CO_2 \text{ laser}]{SF_6, H_2}$ **Si nanoparticles**

(oxide embedded, d ~ 5 nm)

C.

SiO_X $\xrightarrow[\substack{2 \text{ hours}}]{1000°C, \text{ Ar}}$ **Si nanoparticles**

X = 0.4, 1.0, or 1.6 (oxide embedded, d = 5.1 ± 1.87 nm)

D.

[HSQ cage structure] $\xrightarrow[\substack{1000°C, \; 1 \text{ hour}}]{4\% \; H_2/96\% \; N_2}$ **Si nanoparticles**

(oxide embedded, d = 2.3 ± 0.25 nm)

Scheme 4 Solution-, solid- and gas-phase molecular precursor thermolysis preparation of freestanding silicon nanocrystals.

(*ca. d* = 30–80 nm) octahedral Si single crystals was reported by first reported by Murthy *et al.*[34] This pivotal development has been built upon by numerous researchers. In particular, Brus *et al.* used a modification of this method to control the size of oxide capped FS-*nc*-Si and subsequently provided significant insight into the optical properties of silicon nanostructures including *p*-Si and FS-*nc*-Si (*vide infra*).[9,35]

A variation of the silane pyrolysis that used a CO_2 laser to decompose the silicon precursor was first reported in 1982 by Cannon *et al.*[36] and afforded gram quantities of agglomerated Si particles. Products from these early studies showed no PL behavior. Minor procedural variants were employed by numerous groups.[37] Still, only Huisken *et al.* reported significant PL response upon etching their product with HF.[38]

In 2003, Swihart and coworkers reported the use of laser induced SiH_4 pyrolysis as an efficient method for preparing large quantities of Si nanoparticles at rates of 20–200 mg h^{-1}(Scheme 4B). FS-*nc*-Si obtained from of this procedure had particle dimensions of *ca.* 5 nm. These particles exhibit tunable photoluminescence (external quantum efficiency 0.5–10%) spanning the visible spectrum upon controlled etching with HNO_3–HF and are amenable to surface functionalization (*vide infra*).[39–42]

Silicon sub-oxides have long been used to prepare thin films of silicon rich oxides (SRO) consisting of silicon nanoparticles within a SiO_2.[11] Recently, Liu *et al.*[43,44] exploited this well-established thin film precursor and prepared solution borne FS-*nc*-Si upon HF or HF–HNO_3 etching of the product obtained from thermal annealing of commercially available SiO_X (X = 0.4–1.8) in flowing argon at 900 °C (Scheme 4C). It was confirmed by TEM that the product of the HF etching procedure was 4.2 nm diameter (polydispersity of 12%) nanophase diamond lattice Si and was supported XRD.

Particle surfaces were confirmed to be hydride terminated by FT-IR. No yield data were provided.

Commercially available hydrogen silsesquioxine (HSQ) has been found by Hessel *et al.* to quantitatively decompose thermally to yield thin film and bulk quantities of SROs (Scheme 4D). Upon HF etching hydride surface terminated FS-*nc*-Si are liberated.[45] While the exact mechanism of the thermal decomposition of HSQ remains unclear, it is believed that the cage structure collapses producing two SiH_4 molecules for every HSQ unit at *ca.* 410 °C. During rapid heating, the liberated silane becomes trapped in the rapidly forming Si–O matrix and decomposes at 450 °C[46] to form nanocrystalline silicon particles. Highly photoluminescent, FS-*nc*-Si (*d* = 3.41 ± 1.40 nm) of tunable emission maxima are obtained from HF etching as a orange powder and have been confirmed to be hydride surface terminated by FT-IR analysis.

Physical methods

Perhaps the most widely studied Si-based nanostructure is porous silicon (*p*-Si).[8] While this material and its chemistry are beyond the scope of the present contribution, it is important to note that examples of FS-*nc*-Si prepared *via* pulverizing and sonicating *p*-Si are found in the scientific literature.[47–50] These highly luminescent powders are obtained in small quantities and have provided fundamental insight into the properties of FS-*nc*-Si. Published data indicate they are not individual Si nanoparticles, but are *nc*-Si domains trapped in larger (*i.e.*, ≥ 1 µm) pieces of the *p*-Si structure.

Summary FS-*nc*-Si preparative methods

Clearly, significant advances in the preparation of FS-*nc*-Si have been realized in the past thirteen years. A variety of FS-*nc*-Si species bearing chemically active surfaces and materials showing high PL external quantum yields have been prepared using solution chemistry. In addition, methods exist for preparing large quantities of FS-*nc*-Si and some ability to tailor shape has been demonstrated. Still, challenges remain. While it appears that all the criteria of an ''ideal'' preparative method have been realized, no single method fulfills all the pertinent issues simultaneously (*vide supra*). In addition, two important issues that remain are the reliance of many of existing methodologies on specialized reagents/reactors as well as the need for somewhat hazardous HF or HF–HNO_3 to afford efficient control over particle size.

3. Controlling particle surface chemistry

A very important attribute of nanoparticles is their enormous surface area to volume ratio. Highlighting this property, one may consider the estimate that a 2.0 nm diameter icosahedral silicon particle is made up of approximately 280 Si atoms with 120 (43%) residing at the particle surface.[40] Surface chemistry has already been shown to impact on the optical properties of *p*-Si.[51] Computationally, it has been predicted that surface chemistry will greatly influence the lowest unoccupied molecular orbital (LUMO) energy and hence the optical band gap of very small FS-*nc*-Si.[26,52] In this regard, FS-*nc*-Si surface chemistry is an essential property that must be controlled if

these materials are to be fully understood and their applications realized.

To date, surface chemistry has been shown to render FS-*nc*-Si more stable toward oxidation, increase "solubility" in a variety of solvents and has offered convenient methods for particle purification, influencing particle electronic structure, and very recently provided a convenient method for controlling particle optical response *via* what has been suggested to be controlled oxidation.

The earliest synthetic reports on FS-*nc*-Si, while making no attempt to tailor particle surface chemistry, noted its complexity,[13,14] while others confined their study to well-defined oxide surface termination.[9,35] Later reports of FS-*nc*-Si synthesis *via* thermolysis of diphenylsilane in supercritical solvents also indicated particle surfaces were complex and that the phenyl substituents present in the molecular precursors did not remain on particle surfaces. Following synthesis, however, the presence of octanethiol in the reaction mixture seemed to result in organic monolayer stabilization.[30,31] All of these early observations underscore the challenges associated with and the importance of particle air sensitivity and post synthetic derivatization if particles of well-defined, diverse surface chemistry were to be realized.

One key factor in tailoring surface chemistry is the realization of a chemically active surface (*e.g.*, Si–Cl, Si–Br, Si–H, Si–OH) that allows subsequent derivatization. The surface chemistry of bulk silicon surfaces is a well-developed field of study and serves as a foundation for most functionalized FS-*nc*-Si studies.[8] One of the earliest examples of FS-*nc*-Si surface reactions is particle capping with methoxy surface functionalities during the post-synthetic methanol workup of the product mixture obtained from potassium silicide reduction of SiCl$_4$. The proposed surface reaction is shown in Scheme 5A. While definitive data confirming chloride surface termination could not obtained, spectroscopic data supported the conclusion that the air stable, hydrophobic product was in fact –OCH$_3$ surface terminated.[16] Particles obtained from Zintl salt reactions have also been derivatized using alkyl lithium and Grignard reagents (Scheme 5A), as well as lithium aluminium hydride (Scheme 5A) and bromine (Scheme 5A) all highlighting the breadth of surface reactivity supported by the presence of chloride moieties.[17–20,28] Similar surface reactivity was also observed for particles obtained from sodium naphthalide reduction of SiCl$_4$.[24,25]

Stepwise particle surface termination has lead to an "ultrastable" siloxane capped product (Scheme 5A). Silicon particles were initially terminated with methoxy moieties upon exposure to methanol that were reacted with alkyl trihydroxysilanes to yield particles with crosslinked siloxane surfaces. This same product was also obtained *via* a second route in which the alkoxy groups were replaced by reactive –OH moieties upon exposure to water followed by further reaction with an alkyl trichlorosilane.[26] This series of reactions effectively demonstrated that the surfaces of FS-*nc*-Si can serve as a reaction substrate and could lead to the incorporation of *indirect bandgap* semiconductor particles into functional materials.

As noted previously, laser induced pyrolysis of SiH$_4$ produces loosely agglomerated FS-*nc*-Si encapsulated in an
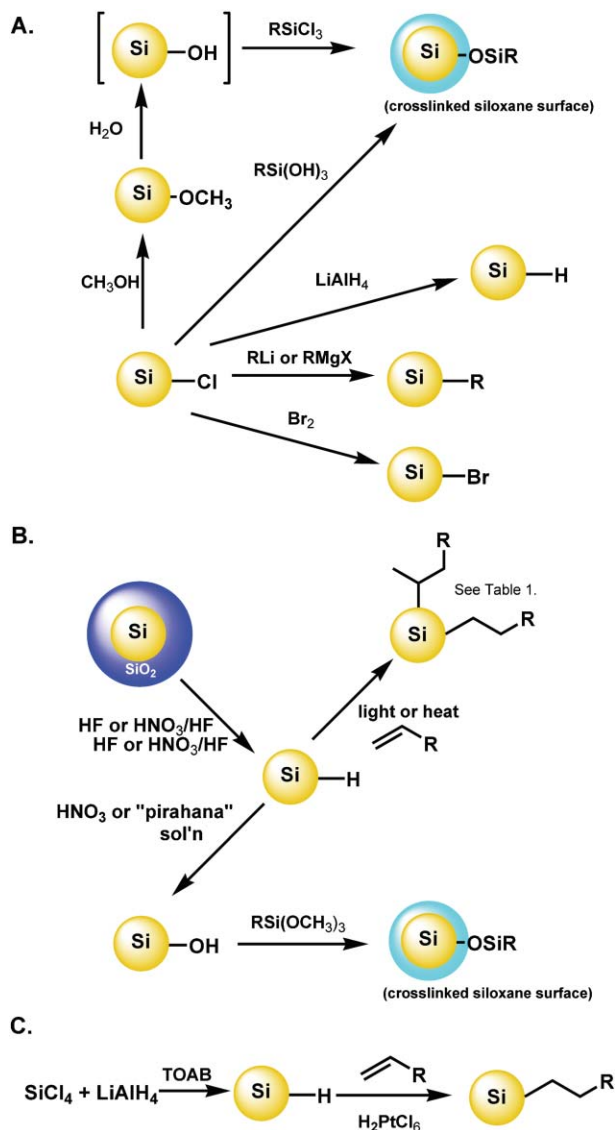
Scheme 5 Solution methods for tailoring FS-*nc*-Si surface chemistry.

amorphous material that doubtless consists of silicon oxides. The raw product was effectively treated with mixtures of HF and HNO$_3$ to produce a hydride surface terminated by FS-*nc*-Si (Scheme 5B).[42] Thermo- and photochemically initiated hydrosilylation (Scheme 5B) have proven effective methods for rendering these particles hydrophobic, soluble in organic solvents (Fig. 2) and somewhat stable toward oxidation ultimately stabilizing particle optical response.[41,44] For photochemically induced hydrosilylation of FS-*nc*-Si surfaces, the organic surface cap was found to attach *via* the α and β carbons depending upon the steric bulk of the capping ligand (Table 1). This reaction selectivity was effectively tracked using solution ^{1}H NMR that confirmed the reaction favored α and β attachment for large and small alkenes, respectively. Similar observations were not reported for the thermally initiated reaction.

Tilley *et al.* also reported hydrosilylation surface functionalization of the tetraoctylammonium bromide (TOAB) stabilized product obtained from the LiAlH$_4$ reduction of SiCl$_4$.
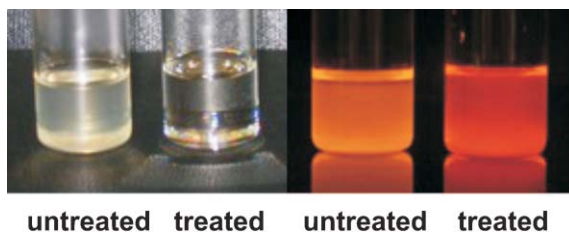
Fig. 2 Untreated and octadecene-treated samples under room illumination (two pictures on the left) and UV illumination (two pictures on the right). Reprinted with permission from reference 39. Copyright 2006 American Chemical Society.

Table 1 Structural dependence of photochemical ligand surface reactivity

Ligand	Mole fraction reaction at terminal carbon[a]
1-Pentene	0.387
1-Hexene	0.399
1-Octene	0.451
1-Dodecene	0.630
1-Octadecene	0.639

[a] Determined from ^{1}H NMR integration ratios for surface functionalized particles.[40]

Upon stirring at room temperature with terminal alkenes and catalytic amounts of hexachloroplatinic acid particle surfaces were derivatized with a variety of functional groups including heptane and allylamine.[23]

Hydride surface terminated particles obtained from etching of SiH$_4$ laser pyrolysis have also been converted to Si–OH surface functionalities using two methods, exposure to 20% nitric acid or a "piranha" etch (Scheme 5B).[41] This surface conversion opens the possibility of modifying the particle surface using organotrichlorosilanes (*vide supra*) and has already afforded the covalent incorporation of FS-*nc*-Si into a conductive polymer matrix.[53]

4. Optical properties response of FS-*nc*-Si

As is the case with other silicon nanomaterials (*e.g.*, *p*-Si and SROs), perhaps the most obvious and intriguing property that arises upon reduction of particle size is the observed visible photoemission not commonly seen in bulk Si. (Bulk Si exhibits a sharp emission line at 1060 nm when cooled to liquid helium temperatures.)[9b] In addition, FS-*nc*-Si particles have exhibited electrochemiluminesence.[7] While the optical properties of other Si nanomaterials are often dominated by a photoluminescent maximum at approximately 1.7 eV, this is not strictly the case for FS-*nc*-Si. Relatively wide size distributions of FS-*nc*-Si particles exhibit excitation wavelength dependent PL maxima (Fig. 3)[19,20,26,29] and size-selected samples can exhibit emission spanning the visible spectrum (Fig. 4)[40] with PL quantum yields ranging from a few percent to as high as 23%.[30]

Some researchers suggest that the PL of Si nanostructures arises because the bandgap transition becomes weakly dipole allowed in this size regime.[54] Others claim that the photoemission originates from the passivation of surface traps present in bulk Si.[55] To date, methods for relating PL energy maximum
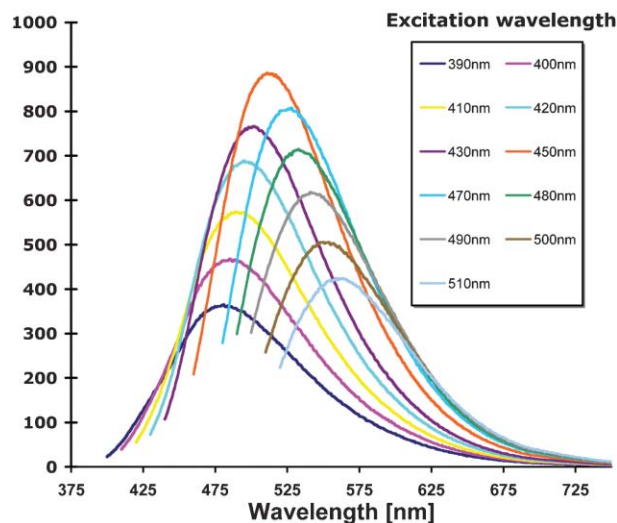

Fig. 3 Excitation wavelength dependence of the PL spectra for size polydisperse trioctylphosphine oxide stabilized FS-*nc*-Si. Adapted from ref. 29.
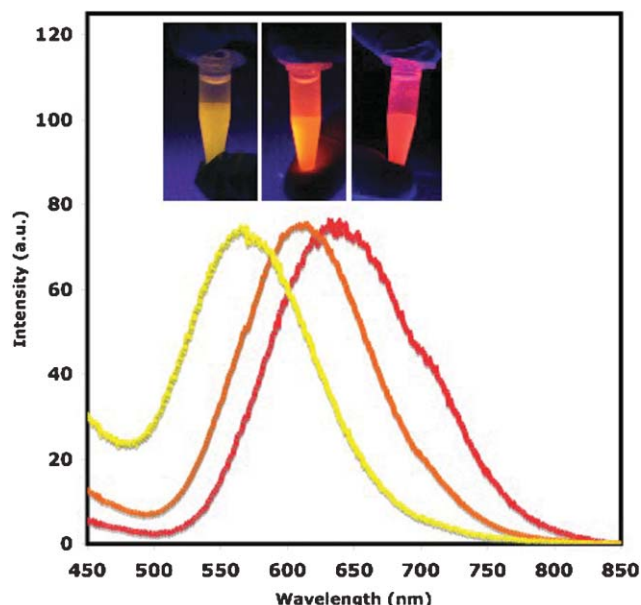

Fig. 4 Normalized emission spectra of different sizes of hydride terminated silicon nanoparticles (λ_{ex} = 350 nm). Size controlled particles were isolated from *nc*-Si/SiO$_2$ prepared by thermally processing hydrogen silsesquioxane upon timed etching in ethanol–water solutions of HF (red 250 min, orange 85 min, yellow 115 min).

to particle size are diverse and a variety of models have been proposed including the effective mass approximation,[56] empirical tight binding band theory,[57,58] empirical pseudopotential approximation,[59,60] and *ab initio* local density approximation.[52,61,62] A full discussion of these investigations is beyond the scope of the present manuscript.

Recent computational and experimental results add to our understanding while also pointing to the complexity of FS-*nc*-Si optical response and quantum confinement. These reports indicate that particle size and surface chemistry influence

independently and in concert if *indirect* and *direct* bandgap behavior is observed.[23,30,63,64]

Brus *et al.* provided a detailed discussion of the PL behavior of size-selected (d = 1–10 nm), oxide surface-terminated FS-*nc*-Si prepared *via* a high temperature aerosol reaction.[9a,9b,35] They reported that FS-*nc*-Si particles exhibited absolute emission quantum yields (QY) of 4–5% (300 K) that increase to 20–50% upon cooling to below 50 K. Single exponential fitting of time resolved emission data showed average lifetimes (τ) of 50 μs (293 K) and 2.5 ms (20 K). These data were explained in the context of unimolecular decay of the electron–hole pair *via* two competing mechanisms; Γ_r (radiative) and Γ_{nr} (non-radiative). Hence, $\tau^{-1} = \Gamma_r + \Gamma_{nr}$ and QY = $\Gamma_r/(\Gamma_r + \Gamma_{nr})$. It was found that at low temperatures (<50 K) the intensity remained constant and the lifetime continued to increase. Hence, the conclusion was made that at low temperatures decay was dominated by radiative decay mechanisms and that any deviation from a 100% QY arose from the influence of non-perfect crystallites with emission quenching defects. The observation of a broadened absorption spectrum added further support to the conclusion that FS-*nc*-Si behave as indirect gap materials and that radiationless decay shortens lifetimes and lowers luminescent quantum yields.

In this same study of oxide surface terminated FS-*nc*-Si, the authors also noted a striking difference between the optical properties of *direct* and *indirect* bandgap semiconductor nanoparticles - the absence of discrete transitions in the FS-*nc*-Si optical spectra. Holmes *et al.* observed these discrete energy transitions in the PL spectra of very small ($d \approx 1.5$ nm) particles; however, only broad emission was noted for larger systems (d = 2.5–40 nm) suggesting size-dependent bandgap characteristics for these materials (*vide infra*).[30] Holmes also reported the highest room temperature PL quantum yields to date for FS-*nc*-Si at 23% and attributed this to the high efficiency with which the supercritical fluid technique passivated particle surfaces. Still, the absorption coefficient increased quadratically with incident energy, $\alpha \approx [h\nu - E_g]$, near the absorption edge further supporting the conclusions made previously by Brus *et al.* of a predominantly indirect gap transition.

In 2003, Brus *et al.*[63] added to our understanding with a computational report that offered further insight in the optical behavior of FS-*nc*-Si outlined in a series of experimental reports claiming, in the absence of conclusive characterization, that ultrasmall (*i.e.*, 1.1–1.4 nm) hydride surface terminated FS-*nc*-Si are dominated by blue emission and a direct gap transition.[23,30,63] This observation is very different from what was previously noted for oxide terminated particles of equivalent size particles that show a dipole forbidden red–yellow emission and similar to what was experimentally demonstrated by Wolkin *et al.* for blue emitting hydride terminated nanocrystals in p-Si red-shifted upon oxidation.[51] Importantly, this observation appears to contradict simple quantum confinement because the Si particle core size decreases as a result oxidation while the corresponding emission maximum decreases in energy.

Brus *et al.* compared the theoretical electronic structure of hydride surface terminated Si_{35} (d = 1.1 nm) and Si_{66}

(d = 1.4 nm) particles of T_d symmetry using DFT methods with unrestricted geometry optimization. They noted that anionic and neutral $Si_{35}H_{36}$ and $Si_{66}H_{64}$ all retain T_d symmetry after complete geometry optimization. For the octahedral $Si_{35}H_{36}$ fragment with exposed 111 facets, the excited state resides at the particle surface. As the particle increases in size (*i.e.*, $Si_{66}H_{64}$) the excited state wavefunctions become less surface localized. In both cases, the highest occupied molecular orbital (HOMO) and lowest unoccupied molecular orbital remained delocalized thereby eliminating the possibility of high energy surface defect mediated emission. Still, for both these particles there are six single-electron transitions calculated to be close to the bandgap making it very likely that the transition will be electric-dipole allowed.

In contrast, when the optical properties of equivalent particles bearing a pseudo-oxide termination (*i.e.*, –OH) were computed for $Si_{35}(OH)_{36}$ fragments with T_d symmetry a large decrease in *bandgap* energy was noted and the symmetry of the HOMO changed leading to a dipole-forbidden bandgap transition. These calculations also indicated that the bandgap difference between hydride and oxide terminated particles decreases with increased particle size (*i.e.*, $Si_{35} \rightarrow Si_{66}$). The authors suggested that as particle size increases there will be an intermediate size regime in which size and surface chemistry effects will offset and in large particles size effects will dominate with wavefunctions approaching those of simple quantum confinement.

5. Conclusions and outlook

From the body of work outlined herein, it is clear that FS-*nc*-Si research has advanced significantly during the past 1½ decades. Efficient methods for material preparation bearing a variety of reactive surfaces will lead to a better understanding of the fundamental properties of silicon nanostructures including the size dependent PL properties of indirect gap semiconductor nanoparticles. Modern synthetic and derivatization protocols afford macroscopic quantities of material that will doubtless facilitate the integration FS-*nc*-Si with other chemical systems or the use these particles as precursors for functional materials.

It is very difficult to accurately predict the future direction of a field of research. Still, in the light of the unique chemical, optical, and electronic properties of FS-*nc*-Si it is clear that their impact will be far reaching and diverse. Without question, the scientific community will continue to strive to develop synthetic procedures that do not require hazardous material handling and increase our understanding of the optical and electronic properties of Si nanostructures. Other potential avenues of research may include, effective, targeted *in vivo* sensing not readily accessible with toxic compound semiconductors, organic light emitting diodes and light harvesting devices, doped Si nanoparticle inks for fabrication of small semiconductor patterns and devices, and even the remote possibility of alternative fuel storage. Without question, the field of FS-*nc*-Si remains a growing and diverse scientific niche that, with the input of creative researchers will have a significant impact on society.

Acknowledgements

References

1 (a) L. E. Brus, *Appl. Phys. A*, 1991, **53**, 465–474; (b) A. P. Alivisatos, *Science*, 1996, **271**, 933–937.
2 (a) Y. Wang and N. Herron, *J. Phys. Chem.*, 1991, **95**, 525–532; (b) H. Weller, *Angew. Chem., Int. Ed. Engl.*, 1993, **32**, 41–53.
3 A. D. Yoffe, *Adv. Phys.*, 2001, **50**, 1–208.
4 (a) L. Manna, E. C. Scher and A. P. Alivisatos, *J. Am. Chem. Soc.*, 2000, **122**, 12700–12706; (b) B. O. Dabbousi, J. Rodriguez-Viejo, F. V. Mikulec, J. R. Heine, H. Mattoussi, R. Ober, K. F. Jensen and M. G. Bawendi, *J. Phys. Chem. B*, 1997, **101**, 9463–9475.
5 (a) M. C. Schlamp, X. G. Peng and A. P. Alivisatos, *J. Appl. Phys.*, 1997, **82**, 5837–5842; (b) D. L. Klein, R. Roth, A. K. L. Lim, A. P. Alivisatos and P. L. McEuen, *Nature*, 1997, **389**, 699–701; (c) L. S. Li and A. P. Alivisatos, *Adv. Mater.*, 2003, **15**, 408–411; (d) W. U. Huynh, J. J. Dittmer and A. P. Alivisatos, *Science*, 2002, **295**, 2425–2427; (e) For example see: B. Dubertret, P. Skourides, D. J. Norris, V. Noireaux, A. H. Brivanlou and A. Libchaber, *Science*, 2002, **298**, 1759–1762.
6 A. M. Derfus, W. C. W. Chan and S. N. Bhatia, *Nano Lett.*, 2004, **4**, 11.
7 Z. Ding, B. M. Quinn, S. K. Haram, L. E. Pell, B. A. Korgel and A. J. Bard, *Science*, 2002, **296**, 1293–1297.
8 J. M. Buriak, *Chem. Rev.*, 2002, **102**, 1271–1308.
9 (a) L. Brus, *J. Phys. Chem.*, 1994, **98**, 3575–3581; (b) K. A. Littau, P. J. Szajowski, A. J. Muller, A. R. Kortan and L. E. Brus, *J. Phys. Chem.*, 1993, **97**, 1224–1230.
10 (a) J. D. Meindl, Q. Chen and J. E. Davis, *Science*, 2001, **293**, 2044–2049; (b) Y. Cui and C. M. Leiber, *Science*, 2001, **291**, 851–853.
11 A. Meldrum, *Recent Res. Dev. Nucl. Phys.*, 2004, **1**, 93–132.
12 N. N. Greenwood and A. Earnshaw, *Chemistry of the Elements*, Pergamon Press, New York, 1984.
13 J. R. Heath, *Science*, 1992, **258**, 1131–1133.
14 N. A. Dhas, C. P. Raj and A. Gedanken, *Chem. Mater.*, 1998, **10**, 3278–3281.
15 R. K. Baldwin, J. Zou, K. A. Pettigrew, G. J. Yeagle, R. D. Britt and S. Kauzlarich, *Chem. Commun.*, 2006, 658–660.
16 R. A. Bley and S. M. Kauzlarich, *J. Am. Chem. Soc.*, 1996, **118**, 12461–12462.
17 D. Mayeri, B. L. Phillips, M. P. Augustine and S. M. Kauzlarich, *Chem. Mater.*, 2001, **13**, 765–770.
18 C.-S. Yang, R. A. Bley, S. M. Kauzlarich, H. W. H. Lee and G. R. Delgado, *J. Am. Chem. Soc.*, 1999, **121**, 5191–5195.
19 Q. Liu and S. M. Kauzlarich, *Mater. Sci. Eng., B*, 2002, **B96**, 72–75.
20 K. A. Pettigrew, Q. Liu, P. Power and S. M. Kauzlarich, *Chem. Mater.*, 2003, **15**, 4005–4011.
21 A. E. Finholt, A. C. Bond and H. I. Schlesinger, *J. Am. Chem. Soc.*, 1947, **69**, 1199–1203.
22 J. P. Wilcoxon and G. A. Samara, *Appl. Phys. Lett.*, 1999, **74**, 3164–3166.
23 (a) J. H. Warner, H. Rubinsztein-Dunlop and R. D. Tilley, *J. Phys. Chem. B*, 2005, **109**, 19064–19067; (b) J. H. Warner, A. Hoshino, K. Yamamoto and R. D. Tilley, *Angew. Chem., Int. Ed.*, 2005, **44**, 4550–4554; (c) R. D. Tilley, J. H. Warner, K. Yamamoto, I. Matsui and H. Fujimori, *Chem. Commun.*, 2005, 1833–1835.
24 R. K. Baldwin, K. A. Pettigrew, E. Ratai, M. P. Augustine and S. M. Kauzlarich, *Chem. Commun.*, 2002, 1822–1823.
25 R. K. Baldwin, K. A. Pettigrew, J. C. Garno, P. P. Power, G.-y. Liu and S. M. Kauzlarich, *J. Am. Chem. Soc.*, 2002, **7**, 1150–1151.
26 J. Zou, R. K. Baldwin, K. A. Pettigrew and S. M. Kauzlarich, *Nano Lett.*, 2004, **4**, 1181–1186.
27 S. Lee, W. J. Cho, I. K. Han, W. J. Choi and J. I. Lee, *Phys. Status Solidi B*, 2004, **241**, 2767–2770.
28 S. Lee, W. J. Cho, C. S. Chin, I. H. Han, W. J. Choi, Y. J. Park, J. D. Song and J. I. Lee, *Jpn. J. Appl. Phys.*, 2004, **43**, L784–L7896.
29 B. D. Rowsell and J. G. C. Veinot, *Nanotechnology*, 2005, **16**, 732–736.
30 J. D. Holmes, K. J. Ziegler, R. C. Doty, L. E. Pell, K. P. Johnston and B. A. Korgel, *J. Am. Chem. Soc.*, 2001, **123**, 3743–3748.
31 D. S. English, L. E. Pell, Z. Yu, P. F. Barbara and B. A. Korgel, *Nano Lett.*, 2002, **2**, 681–686.
32 (a) D. C. Lee, T. Hanrath and B. A. Korgel, *Angew. Chem., Int. Ed.*, 2005, **44**, 3573–3577; (b) H.-Y. Tuan, D. C. Lee, T. Hanrath and B. A. Korgel, *Nano Lett.*, 2005, **5**, 681–684; (c) X. Lu, T. Hanrath, K. P. Johnston and B. A. Korgel, *Nano Lett.*, 2003, **3**, 93–99; (d) J. D. Holmes, K. P. Johnston, R. C. Doty and B. A. Korgel, *Science*, 2000, **287**, 1471–1473.
33 L. E. Pell, A. D. Schricker, F. V. Mikulec and B. A. Korgel, *Langmuir*, 2004, **20**, 6546–6548.
34 T. U. M. S. Murthy, N. Miyamoto, M. Shimbo and J. Nishizawa, *J. Cryst. Growth*, 1976, **33**, 1–7.
35 W. Wilson and L. E. Brus, *Science*, 1993, **262**, 1242–1244.
36 W. R. Cannon, S. C. Danforth, J. H. Flint, J. S. Haggerty and R. A. Marra, *J. Am. Ceram. Soc.*, 1982, **65**, 324–330; W. R. Cannon, S. C. Danforth, J. S. Haggerty and R. A. Marra, *J. Am. Ceram. Soc.*, 1982, **65**, 330–335.
37 E. Borsella, S. Botti, M. Cremona, S. Martelli, R. M. Montreali and A. Nesterenko, *J. Mater. Sci. Lett.*, 1997, **16**, 221–223; S. Botti, R. Coppola, F. Gourbilleau and R. Rizk, *J. Appl. Phys.*, 2000, **88**, 3396–4836.
38 G. Ledoux, J. Gong, F. Huisken, O. Guillois and C. Reynaud, *Appl. Phys. Lett.*, 2002, **80**, 4834–4836; G. Ledoux, J. Gong and F. Huisken, *Appl. Phys. Lett.*, 2001, **79**, 4029–4030; F. Huisken, B. Kohn and V. Paillard, *Appl. Phys. Lett.*, 1999, **74**, 3776–3778.
39 F. Hua, F. Erogbogbo, M. T. Swihart and E. Ruckenstein, *Langmuir*, 2006, **22**, 4363–4370.
40 F. Hua, M. T. Swihart and E. Ruckenstein, *Langmuir*, 2005, **21**, 6054–6062.
41 X. Li, Y. He and M. T. Swihart, *Langmuir*, 2004, **20**, 4720–4727.
42 X. Li, Y. He, S. S. Talukdar and M. T. Swihart, *Langmuir*, 2003, **19**, 8490–8496.
43 S.-M. Liu, Y. Yang, S. Sato and K. Kimura, *Chem. Mater.*, 2006, **18**, 637–642.
44 S.-M. Liu, S. Sato and K. Kimura, *Langmuir*, 2005, **21**, 6342–6329.
45 C. Hessel, E. J. Henderson and J. G. C. Veinot, *Chem. Mater.*, 2006, submitted.
46 T. R. Hogness, T. L. Wilson and W. C. Johnson, *J. Am. Chem. Soc.*, 1947, **69**, 1199–1203.
47 G. Belomoin, J. Therrien, A. Smith, S. Rao, R. Twesten, S. Chaleb, M. H. Nayfeh, L. Wagner and L. Mitas, *Appl. Phys. Lett.*, 2002, **80**, 841–843.
48 M. H. Nayfeh, N. Barry, J. Therrien, O. Akcakir, E. Gratton and G. Belomoin, *Appl. Phys. Lett.*, 2001, **78**, 1131–1133.
49 M. H. Nayfeh, O. Akcakir, G. Belomoin, N. Barry, J. Therrien and E. Gratton, *Appl. Phys. Lett.*, 2000, **77**, 4086–4088.
50 R. A. Bley, S. A. Kauzlarich, J. E. Davis and H. W. H. Lee, *Chem. Mater.*, 1996, **8**, 1881–1888.
51 (a) J. M. Laurerhaas and M. J. Sailor, *Science*, 1993, **261**, 1567–1568; (b) M. V. Wolkin, J. Jorne, P. M. Fauchet, G. Allan and C. Delerue, *Phys. Rev. Lett.*, 1999, **82**, 197–200.
52 F. A. Reboredo and G. Galli, *J. Phys. Chem. B*, 2005, **109**, 1072.
53 Z. F. Li, M. T. Swihart and E. Ruckenstein, *Langmuir*, 2004, **20**, 1963–1971.
54 T. Takagahara and K. Takeda, *Phys. Rev. B*, 1992, **46**, 15578–15581.
55 V. I. Klimov, C. J. Schwarz, D. W. McBranch and C. W. White, *Appl. Phys. Lett.*, 1998, **73**, 2603–2605.
56 M. Breitenecker, R. Sexl and W. Thirring, *Z. Phys.*, 1964, **182**, 123.
57 N. A. Hill and K. B. Whaley, *J. Electron. Mater.*, 1996, **25**, 269–285.
58 N. A. Hill and K. B. Whaley, *Phys. Rev. Lett.*, 1995, **75**, 1130–1133.

59 L. W. Wang and A. Zunger, *J. Phys. Chem.*, 1994, **98**, 2158–2165.

60 C. Delerue, G. Allan and M. Lannoo, *Phys. Rev. B*, 1993, **48**, 11024–11036.

61 C. Delerue, G. Allan and M. Lannoo, *J. Lumin.*, 1998, **80**, 65–72.

62 S. Ogut, J. R. Chelikowsky and S. G. Louie, *Phys. Rev. Lett.*, 1997, **79**, 1770–1773.

63 Z. Zhou, L. Brus and R. Friesner, *Nano Lett.*, 2003, **3**, 163–167.

64 G. Belmoin, E. Rogozhina, J. Therrien, P. V. Braun, L. Abuhassan, M. H. Nayfeh, L. Wagner and L. Mitas, *Phys. Rev. B*, 2002, **65**, 193406.